OBSERVATIONS OF MICROSTRUCTURAL AND GEOMETRICAL INFLUENCES ON FATIGUE CRACK GROWTH IN SINGLE CRYSTAL AND POLYCRYSTAL NICKEL-BASE ALLOYS

David C. Wu, David W. Cameron, and David W. Hoeppner

Garrett Engine Division, Allied Signal Aerospace Company,
111 South 34th Street, Phoenix, AZ 85010

115 Clarence Street, Allegany, New York 14706

Chairman, Department of Mechanical and Industrial Engineering,
University of Utah, Salt Lake City, Utah 84112

Abstract

Understanding of single crystal crack growth can yield significant insight into the behavior of similar polycrystalline materials. Two nickel-based alloys which display planar slip under cyclic loading were examined, viz. single crystal SRR 99, and polycrystalline IN 901. The investigations were conducted at ambient temperature using a small load frame integrated with a scanning electron microscope, allowing for both 'still' photographs and dynamic videorecording. Principal goals of the experiments were to observe the nucleation and growth of fatigue cracks under sinusoidal tension-tension loading. The features associated with fracture path development and supplemental fractographic studies are shown for both materials. Orientation-dependent crack growth in the SRR 99 is presented and shown to be a manifestation of Schmid-Law controlled slip. Once this slip is activated, the crack path develops such that the strain energy release rate is maximized. Generally the behavior observed in the single crystal was found in the polycrystal, with allowance for the microstructural variables. The polycrystalline IN 901 displayed responses which reflected the constraint to free slip distance associated with multiply-oriented grains, grain boundaries, eta precipitates, etc. These influences operate to minimize crack extension by a single slip plane which can readily traverse a favorably oriented single grain/crystal. Such 'complexing and hindering' contributes substantially to the fatigue resistance of polycrystalline materials under these conditions.

Superalloys 1988
Edited by S. Reichman, D.N. Duhl,
G. Maurer, S. Antolovich and C. Lund
The Metallurgical Society, 1988

Introduction

The behavior of short cracks under fatigue loading has been a topic of intense interest. One class of short cracks can be termed 'microstructurally-short', i.e. the size of the crack is small with respect to the microstructural unit sizes of the material. It is clear that in this class of short cracks, understanding of single crystal crack growth behavior can yield significant insight into the behavior of similar polycrystalline material.

The studies described in this paper were carried out on two nickel-based superalloys: cast, single-crystal SRR 99 and wrought, polycrystalline IN 901. Both materials display planar slip mode behavior under cyclic loading at room temperature. Principal goals of the studies were the observation of the externally visible circumstances of crack nucleation, the evolution of the crack path as it extended through the material, and the influences of microstructural features.

The SRR 99 alloy, a single crystal turbine blade alloy, was provided in a single bar or block sample grown in the <001> direction. Orientation of the samples was based on reference marks on the block of material whose initial orientation was established by Laue back-reflection techniques. The IN 901 material was obtained from a typical cast and wrought disk for an aeroengine application. No particular directional choices were maintained in this reasonably equiaxed material. The nominal chemistries of the two alloys investigated are given in Table I. Only the principal elements are given in the table, other control limits exist on residual and tramp elements as well.

TABLE I. Alloy Chemistries.

	C	Cr	Co	Mo	Ta	W	Al	Ti	Fe	B	Ni
SRR 99	0.015	8.5	5.0	-	2.8	9.5	5.5	2.2	-	-	bal
IN 901	0.05	13.5	-	6.0	-	-	0.25	2.7	35	0.01	bal

Despite their disparate chemistries and product forms, a substantial number of similar features and events were observed in the experiments.

Experimental Procedure

The experimental apparatus consisted of a servohydraulically-controlled 1.8 kN load frame integrated with an ISI Alpha 9 scanning electron microscope. This facilitated in-situ secondary electron observation and recording of the surface response and cracking processes. Typical 'still' scanning electron micrographs could be taken at any point of the load sequence, and dynamic operation of the system generally ranged from a maximum of 20 to 30 Hz to fractions of a Hertz. These latter frequencies were useful in obtaining dynamic video recordings of events under active loading. Details of the device have been reported previously (1).

The fatigue crack growth experiments were performed using modified single edge notch (SEN) specimens under sinusoidal tension-tension loading. The general specimen geometry is shown in Figure 1; one side of the 1mm thick by 4mm wide gage length was notched to provide the SEN configuration. The test specimen thickness approximated that of cooled airfoil sections

employed in many advanced blade and stator components. In the case of the wrought IN 901, the sample was about 15 grains thick in the through-thickness direction, probably sufficient for a continuum-type response.

Notching of the specimens to obtain the SEN geometry was by mechanical means, e.g. a saw cut. The SRR 99 specimens were first mechanically polished followed by electropolishing to produce a smooth notch root and gage section surface for subsequent observation. Interdendritic porosities, carbides , and gamma prime precipitates were visible at the appropriate magnifications after such surface preparation. The IN 901 specimens were mechanically polished and chemically etched to delineate the grain boundaries and other microstructural features.

The SRR 99 specimens were tested at a load ratio of 0.2, the IN 901 specimens were tested at load ratios of 0.2 and 0.5. Although the applied load ratios were constant, constant load amplitude conditions were not necessarily maintained throughout the test. Common goals of both studies were the observation of the initial circumstances of crack nucleation and the progression of the crack through the microstructure. These two criterion were satisfied by first applying relatively high loads to nucleate crack(s) at the notch root. Following observation of cracking at the root location, the load amplitude was reduced to facilitate more extensive propagation observations, while maintaining the required load ratio.

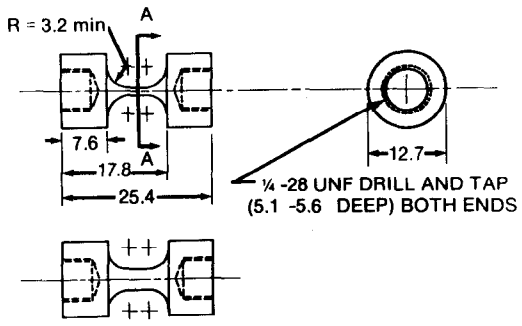

Figure 1 - Specimen geometry. All dimensions mm, except threads.

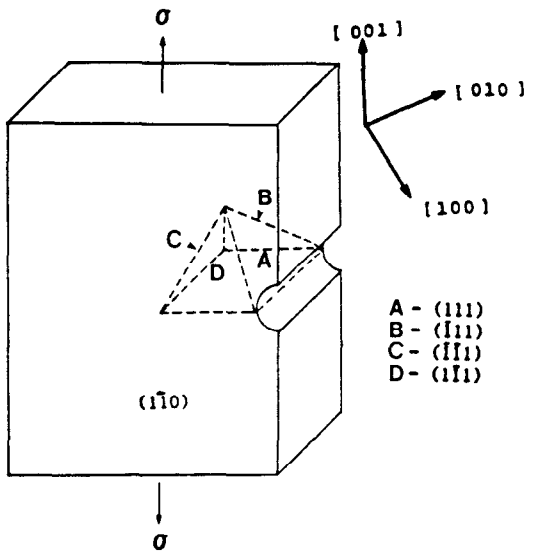

Figure 2 - Relative orientation of the {111} tetrahedron, specimen 4.

Experimental Results

SRR 99 Specimens

Recent studies (2,3) on single crystal nickel-base alloys have shown that at temperatures below approx. 700C, crystallographic cracking on {111} planes predominates under cyclic loading. Preliminary experiments on SRR single crystals confirmed this observation (4). Further experiments on specimens of controlled primary and secondary slip orientations were carried out to define the necessary and sufficient conditions for such crystallographic crack growth. A summary of the specimen orientations tested is shown in Table II.

Table II. SRR 99 Specimen Orientations.

Specimen I.D.	Loading Axis	Specimen Face
1,2	[001]	(100)
3,4	[001]	$(1\bar{1}0)$
5,6	[.12 .12 .986]	"
7,8	$[3\bar{1}0]$	(131)

In all cases, mixed mode I, II, and III cracking was observed. The geometry of the resulting cracks could be visualized based on the relative orientation of the $\{111\}$ tetrahedron with respect to the specimen. The crack nucleation and growth process in all specimens were similar. In all the cases the crack(s) nucleated at material discontinuities in the notch root. Crack evolution in a particularly illustrative specimen will be presented in detail.

The orientation of the $\{111\}$ tetrahedron in specimen 4 is shown in Figure 2. The initial maximum applied net section stress was 475 MPa. At 176,000 cycles, cracking at a pore was observed at the notch root. The maximum applied stress was reduced to 400 MPa and held there until 340,000 cycles, the crack at this point is shown in Figure 3. The applied stress was further reduced in two steps to 250 MPa at 540,000 cycles. Cracking continued at the notch root, a view of it at 1,110,000 cycles is shown in Figure 4. It can be seen that a crack 'branch' has developed.

At 1,160,000 cycles, a fissure appeared on the $(1\bar{1}0)$ face, as shown in Figure 5. This opening was nominally perpendicular to the applied stress and an uncracked ligament remained at the trailing tip of the fissure. A higher magnification view of the opening's leading tip is shown in Figure 6, note the manifestations of slip activity. The fissure remained tight until 1,200,000 cycles, when the trailing tip penetrated the free edge of the specimen.

Figure 3 - Crack nucleation at pore in notch root, N = 340,000 cycles.

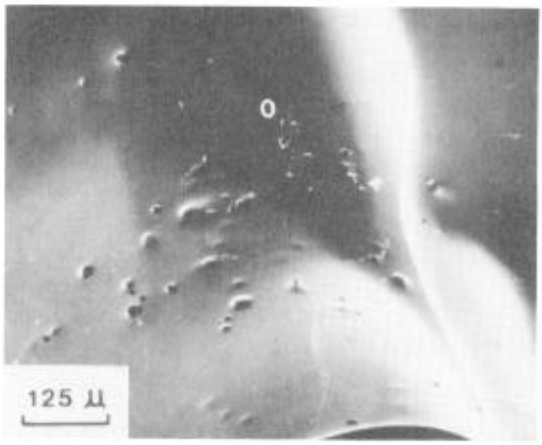

Figure 4 - View of crack at notch root, N = 1,110,000 cycles. Crack branching at nucleating pore indicated by 'O'.

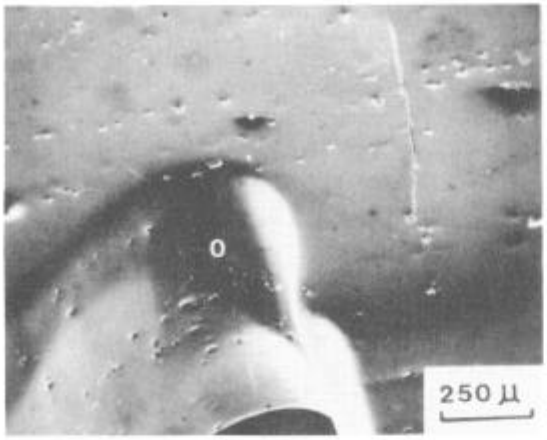

Figure 5 - Notch root and fissure on the free surface, N = 1,160,000 cycles (stress axis horizontal).

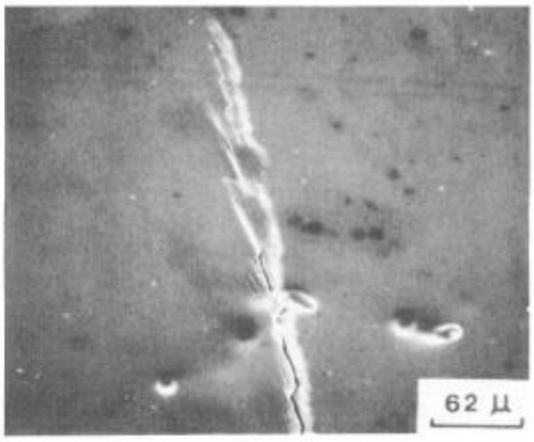

Figure 6 - Leading tip of fissure, N = 1,190,000 cycles.

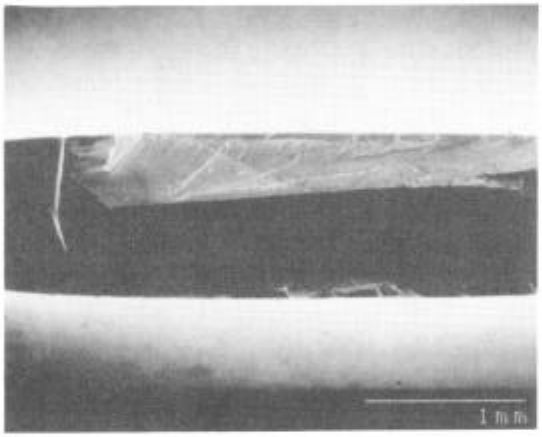

Figure 7 - Plan view of the failed specimen; compare crack geometry to Fig. 2.

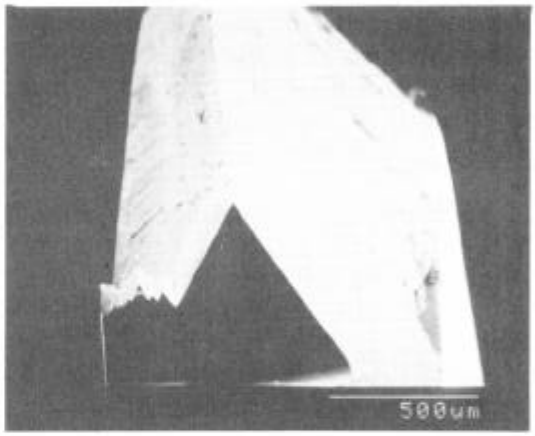

Figure 8 - End-on view from the notch of the failed specimen; compare geometry to Fig. 2.

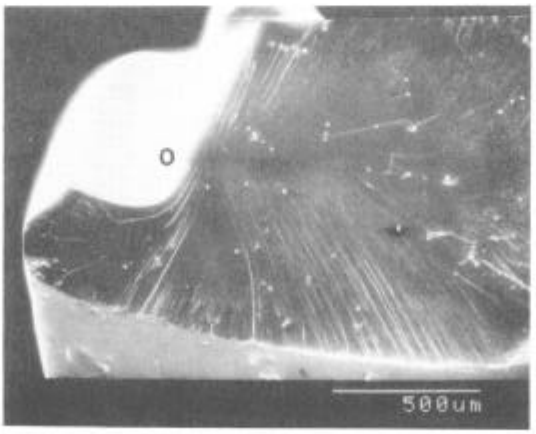

Figure 9 - View of the (111) plane adjacent to notch root. Crack nucleation site shown in Figures 3 to 5 marked by 'O'.

Specimen failure occurred at 1,225,580 cycles. Two views of the separated specimen are shown in Figures 7 and 8. It can be seen that adjacent to the notch, the crack was a three-sided pyramid, as the crack progressed, two sides of the pyramid continued to form a roof-top fracture; all the planes that made up the pyramid and the roof-top were {111} planes. Figure 9 showns the fracture surface on the (111) plane associated with the fissure described earlier. It can be seen that part of the crack had to propagate 'backwards' to complete this particular plane.

Beachmarks and radial ridge lines on Figures 7, 8, and 9 showed simultaneous subsurface cracking on three different planes. This can be explained by the fact that this specimen, with a [001] stress axis, has a multiple slip orientation (eight different octahedral slip systems have the same Schmid factor based on uniaxial loading). Similar behavior in specimens 1 through 3 with the same stress axis had been observed. However, an additional criterion was required to explain the observed crack path.

The crack geometry seen in specimen 4 involved three slip planes initially, but switched to two planes that made up a roof-top. This roof-top approximates a mode I crack. As such, its strain energy release rate is greater than that of a mixed mode I and II crack, which the (111) plane would have formed had it continued to propagate. Using this observation, it was postulated that once slip had been activated according to Schmid's Law, the selection of the crack path is controlled by strain energy release rate considerations: the crack grows along a path that maximizes the strain energy release rate (4).

Specimens 5 through 8 were designed to reduce the number of active slip systems (four in specimens 5 and 6, two in specimens 7 and 8), based on Schmid factor comparison. In both orientations, at least one active slip system was associated with a slip plane that was perpendicular to the broad face of the specimen. If cracking were to continue on that plane, the resulting crack geometry would have been greatly simplified to that of a mixed-mode I & II crack at about 45 degrees to the stress axis, producing unambiguous da/dN crack growth rate data. These through-thickness cracks were not observed. Nevertheless, the actual crack path met the Schmid factor and the maximum strain energy release rate requirements. A generalized version of the energy release rate requirement can be found in reference 5.

IN 901 Specimens

The IN 901 experiments were conducted along with two other materials having markedly different response characteristics (6). The anticipated general planar slip character of the polycrystalline material was manifested early in the tests and continued throughout the area of cyclic crack extension. Initial cracking in all of the samples was controlled by a taper cut notch to force nucleation in the thinned extreme of the notch root, near, if not at, the observed surface of the specimen.

A selection of photos from three tests is included here so that only the most illustrative are present. Control parameters of maximum net section stress and R ratio on these specimens were: sample 1, constant 350 MPa at R = 0.2; sample 2, 400 to 600 MPa at R = 0.5; and sample 5, 400 to 500 MPa at R = 0.2. For reference purposes, total lives of these specimens are: 980,423 cycles, 3,902,662 cycles, and 485,516 cycles, respectively.

Planar slip developed almost immediately after beginning cycling and was reflected in the real-time observations and subsequent fractography (Figure 10). Faceted fracture, very similar to that of the single crystal

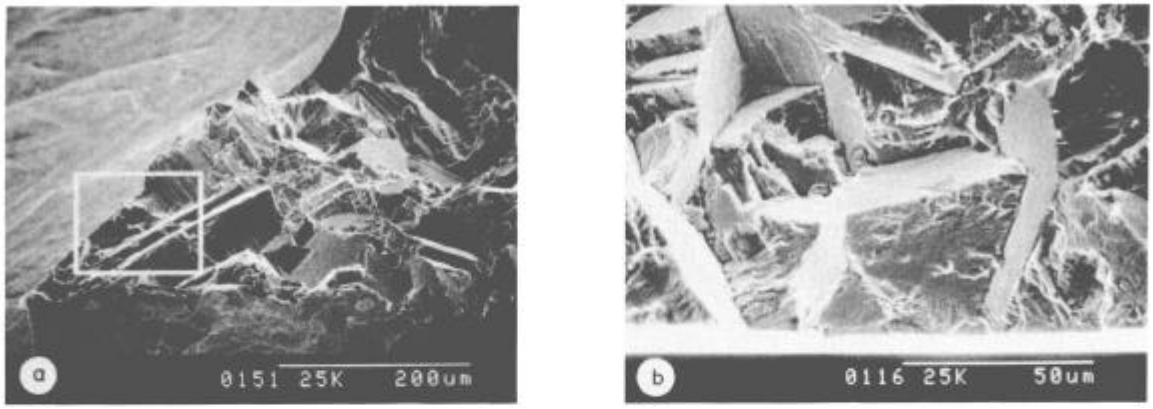

Figure 10 - Fractographs of a) sample 2 and b) sample 1 illustrating the distinctly faceted surfaces.

reported above, including 'roof top' features were found. Very few 'classic' striations were observed. The general character of the facets was similar to that of the single crystal, but the readily observed radiating lines in the SRR 99 were only infrequently seen in the IN 901.

The planar slip character of this polycrystalline material provided for quite varied crack extension responses. In some cases two to four grains would be coupled through mutually compatible, closely oriented slip planes as in sample 2 at 3,250,000 cycles (Figure 11). Within an individual grain these cases frequently gave little evidence of slip on identical, neighboring slip planes of the same orientation, or other related planes. Crack growth was relatively rapid under these circumstances. The other extreme was where multiple octahedral systems were active within an individual grain or where other incompatibilities were present. In such locations relative, local crack extension slowed, reflecting the greater difficulty in extending under these conditions (e.g. Sample 1 at 175,000 cycles, Figure 12).

In the single crystal work described above the extension of cracks 'backwards' was noted. No specific evidence was gathered in the polycrystalline IN 901 to support an identical mechanism, i.e. a crack extending 'backwards' to complete the fracture path to the free surface of the notch root. This is probably due to constraint associated with mean-free-slip path and perhaps notch geometry details. Many times during the real-time

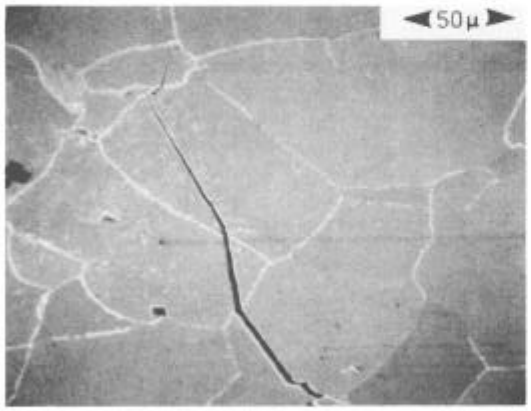

Figure 11 - Multiple grains traversed by a single crack on complementary slip planes (Sample 2, N = 3,250,000 cycles).

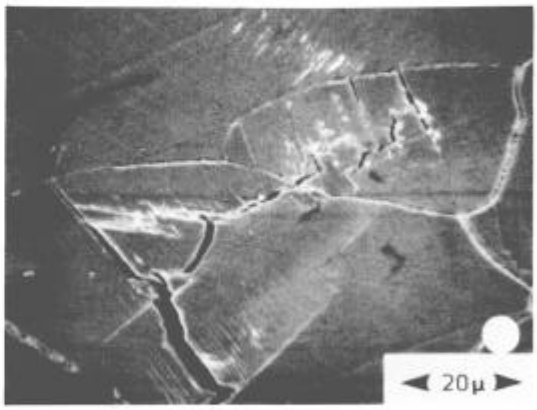

Figure 12 - Diffuse, multiple slip at the crack tip of sample 1, N = 175,000 cycles.

studies of IN 901 cracking was observed 'ahead' of the leading crack tip in locations apparently susceptible to nucleation within the crack tip strain field, e.g. planar slip band crack in a grain, a favorable grain boundary, etc. The general effect is seen in Figure 13 (Sample 5 at 450,000 cycles). The leading cracks would then extend in both directions, forward and backward, until they linked up with the main crack or were by passed by the principal crack front, becoming secondary cracking. Link up did not always occur along slip planes, but might involve grain boundaries, etc.

The eta colonies present in the IN 901 also provided for additional complications of the crack extension response. The presence of the oriented platelets serves to obstruct slip, further shortening the possible mean-free-slip path to an extent sometimes perhaps an order of magnitude less than the grain boundary restriction. This further confounds the cracking and quite tortuous crack paths can develop. One of a series of micrographs reflecting the extension of a crack through an eta colony in the vicintiy of the notch root of specimen number 2 is provided in Figure 14. The platelets were frequently observed to deflect the crack path even where the eta concentration was quite diffuse.

Many other interactions were noted, including: the development of interfering features that correspond to 'roughness' effects, emergence of film-type features from slip bands, rejection of detrital material from between the approximating surfaces, fracture and separation of interfering pieces from along the crack face, etc. These last two items indicate the possibility of crack plane orientation or attitude dependent closure effects. If the movement of debris is 'toward' the crack tip due to potential or other forces, crack tip closure may be inhibited.

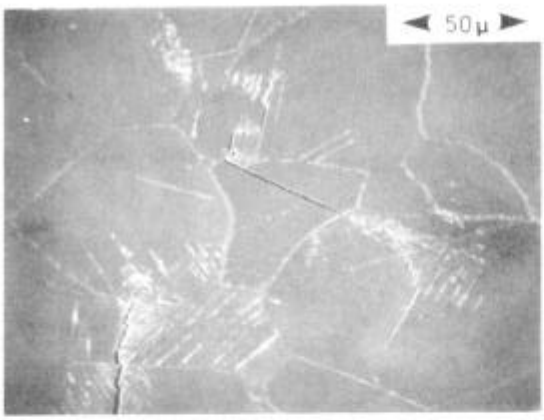

Figure 13 - A fissure 'ahead' of the main crack (Sample 5, N = 450,000 cycles).

Figure 14 - Crack extending through an eta colony in the notch root of sample 2 at 100,000 cycles.

Discussion

At the stress levels employed in this study, most of the initial cracking activities in the single crystal occurred below the observed surface, adjacent to the notch root. Typically, the cyclic life after a well-defined through-thickness crack had developed was less than one-tenth of the cyclic life after detection of crack nucleation. The differential crack growth rate along different portions of the crack front led to uncracked ligaments in the specimen that played an important role in determining crack behavior.

The complexity of the crack front, especially at the early stages of crack growth, gives a direct illustration of the difficulty in unambiguously measuring and characterizing crack growth rate. Testing at higher stress levels would tend to homogenize the crack front at the notch root, however this brings into question whether crack growth rate can be uniquely characterized by K, since the initial crack morphology changes with stress level. Although the measurements of extension were based on surface observations, this difficulty would be encountered no matter which mensuration technique were employed; the specific direction of growth is not part of the information available.

The polycrystalline results illustrate a number of surface and fractographic features similar to the single crystal. The faceted nature of the polycrystal's fractography is a direct reflection of the planar slip response of the material. There was one notable difference between the crystallographic fracture characteristics of the materials. The radiating lines, which were so characteristic of the single crystal SRR 99, were rather uncommon on the IN 901 samples examined; this is remains a puzzle.

The typical nucleation-propagation life fraction observed on the polycrystalline specimens was not consistent with those of the single crystal. This could be due to both the particular method of notching and the more general, inherent 'hinderance and complexing effects' of a polycrystalline microstructure (7).

The original observations and review of the real time recordings revealed local displacements in both materials that were consistent with modes I, II and III. This multiplicity of modes also reflects on the difficulty of K_I as a correlative parameter under some conditions. In cases where local crack displacements are not substantially mode I for general anisotropic reasons (e.g. single crystals) or due to immediate structual alterations (e.g. local grain response in polycrystals), K_I does not apply very well.

The formation of ligaments in both alloys is interesting, even if they both seem to have different origins. This is another area which provides a distinct modelling challenge.

Comparing the fractographic studies to the specimen surface observations revealed the external views to be reasonably reflective of internal specimen response, especially in the IN 901. In addition, there was not a noticeable variation due to the free surface.

Conclusions

Orientation and microstructure-sensitive crack growth in a single crystal and a polycrystalline nickel-base superalloys have been presented. In the case of the single crystal SRR 99, the onset of slip and crystallographic cracking can be predicted by Schmid's law of maximum resolved shear stress. Once cracks are nucleated, the crack path can be shown to be controlled by the strain energy release rate: the crack propagates along a path that maximizes strain energy release rate.

Planar slip was also very obvious in the IN 901 and the predominant form of cracking was by related crystallographic cracking. The polycrystal also showed the influence of other microstructural variables such as grain boundaries, definite indication of slip system dependent grain-to-grain interactions, and the ability of individual precipitates to alter crack path within an eta colony. An individual grains' crystallographic cracking

in IN 901 should be predictable by arguments similar to the preceding paragraph, but is confounded by the polycrystalline structure.

A variety of similarities were observed in the two materials. In a very general sense, the principal difference was polycrystal's constraint of mean free slip path. This behavior is directly related to mixed-orientation grains, their boundaries, and the influence of secondary precipitates.

The applicability of da/dN - (delta) K_I LEFM-type approach is questioned because of the multiplicity of modes present. Further studies are necessary to quantify the effects of various crystallographic constraints that affect crack growth.

Observation of geometrical and microstructural influences on the cracking process highlight the necessity to further define the relativistic issues associated with varying life-prediction approaches for both materials. An additional 'scale' effect is present in the polycrystal alloy: the level of prediction could be the entire specimen/structure or a specific grain at a given location.

Acknowledgements

The experimental efforts reported here were conducted as part of the the Ph.D. dissertations of authors Wu and Cameron at the University of Toronto, Canada. The sponsorship of Rolls-Royce, Plc and the University of Toronto is acknowledged. The assistance of Professor D. McCammond during the latter part of Dr. Wu's studies is also acknowledged.

References

1. D.W. Cameron and D.W. Hoeppner, "A Servohydraulic-Controlled Load Frame for SEM Fatigue Studies," International Journal of Fatigue, 5 (1983) 225-229.

2. C. Howland, "The Growth of Fatigue Cracks in a Nickel-base Single Crystal", The Behaviour of Short Fatigue Cracks, ed K. Miller and E. de los Rios (London, UK: Mechanical Engineering Publications, 1986), 229-239.

3. K. Chan, "Effect of Cross Slip on Crystallographic Cracking In Anisotropic Single Crystals," Acta Metallurgica, 35 (1987), 981-987.

4. D.C. Wu, "An Investigation into the Fatigue Crack Growth Characteristics of a Single Crystal Superalloy" (Ph.D. Thesis, University of Toronto, 1986).

5. J.S. Short, D.W. Hoeppner, and D.C. Wu, "The Maximal Dissipation Rate Criterion II: Analysis of Fatigue Crack Propagation In FCC Single Crystals", Submitted to Engineering Fracture Mechanics, 1988.

6. D.W. Cameron, " Perspectives and Insights on the Cyclic Load Response of Metals" (Ph.D. Thesis, Univeristy of Toronto, 1984).

7. D. McLean, Grain Boundaries in Metals (Oxford, England: Clarendon Press, 1957) 151 ff.